Electronic Supplementary Information (ESI)

Chemical biology suggests pleiotropic effects for a novel hexanuclear copper(II) complex inducing apoptosis in hepatocellular carcinoma cells

Junshuai Zhang,[a] Jiyong Hu,[a] Kun Peng,[b] Wei Song,[a] Shuangcheng Zhi,[a] Endian Yang,[a] Jin'an Zhao,*[ac] Hongwei Hou[c]

a. College of material and chemical engineering, Henan University of Urban Construction, Henan 467036, P.R. China. E-mail: zjinan@zzu.edu.cn

b. Institute of inorganic chemistry, University of Wuerzburg, Bavaria 97074, Germany

c. College of chemistry and molecular engineering, Zhengzhou University, Zhengzhou 450001

1. Materials and Instruments.

All solvents and reagents were of commercial quality (> 95% purity). And all buffer components were of biological grade and used without further purification. Cisplatin was purchased from Shanghai Energy Chemical Co. Ltd. 3-(4,5-dimathylthiazol-2-yl)-2,5-diphenyltetrazolium bromide (MTT), Ethidium bromide (EB), propidium iodide (PI), calf thymus DNA (CT-DNA) were purchased from Sigma-Aldrich Co. (St. Louis, MO, USA). The Annexin V-FITC apoptosis assay kit and cycletest plus DNA reagent kit were obtained from BD Biosciences Inc.(SJ, USA). TMT-6plex isobaric label reagent set was obtained from Thermo Fisher Scientific Inc.

UV-Vis absorption spectra were tested using a Specord 200 UV–visible spectrophotometer. The FT-IR spectra were recorded on a PerkinElmer Frointer spectrophotometer from KBr pellets in the region of 400–4000 cm^{-1}, and the elemental analyses were conducted with elementar Vario MACRO cube analyzer after heated complexes **1** at 180 °C for 24 h under vacuum. Thermogravimetric experiments were performed using a NETZSCH STA 449F3 instrument. MTT assay were measured using a Tecan Infinite M1000 Pro microplate reader. The contents of Cu were determined on an inductively coupled plasma mass spectrometer (ICP-MS) with Nex ION 300X instrument (PerkinElmer, USA). The visualization analysis of comet assays and ROS detection was measured by Zeiss Axio Vert. A1 invert fluorescence microscope. Most flow cytometric analysis was carried out with a Guava easyCyte 6-2I flow cytometer (Millipore, USA), whereas Cell cycle were performed on BD LSR Fortessa TM Cell Analyzer (USA). All nanoLC-MS/MS experiments were performed on a Q Exactive equipped with an Easy n-LC 1000 HPLC system. The MS analysis was performed with Q Exactive mass spectrometer.

2. Synthesis of Complex 1

A mixture of $Cu(NO_3)_2 \cdot 3H_2O$ (0.0072 g, 0.03 mmol), tpbb (0.0070 g, 0.01 mmol), acetonitrile (1 mL), and chloroform (1 mL) was placed in a glass reactor (10 mL) which was heated at 85 °C for 2 days and then gradually cooled to room temperature at a rate of 5 °C/h. Blue crystals of the complex were obtained. Yield: 65% (based on Cu). Elemental Anal. Calcd for $C_{45}H_{33}Cu_3N_{15}O_{18}$ (%): C, 42.81%; H, 2.63%; N, 16.65%; Found (%): C, 42.46%; H, 2.78%; N, 16.42%. IR (KBr/pellet, cm^{-1}): 3432 s, 1605 w, 1481 s, 1438 m, 1384 m, 1276 s, 1167 w, 1008 m, 749 m, 668 w.

3. Crystal Structure Analysis

The single crystal suitable for X-ray determination was selected and mounted on a glass fiber. Diffraction data was recorded on a SuperNova with graphite monochromated Cu-Kα (λ = 1.54184 Å) at 293(2) K. The structure was handled by direct methods and expanded with Fourier techniques. The calculation was conducted with the Olex2 and SHELXL-2018 crystallographic program.[1] All the non-hydrogen atoms were refined anisotropically. The final cycle of full-matrix least-squares refinement was based on the observed reflections and variable parameters. Besides, as the thermal vibration of solvent molecules in complex **1** are extremely large, then removed by the SQUEEZE option of the PLATON software to subtract their contribution to the overall intensity data.[2] Table S1 gives the crystallographic crystal data and structure processing parameters of the complex, and the selected bond lengths and bond angles of it are listed in Table S2. Detailed data for the crystal structure have been deposited with the Cambridge Crystallographic Data Center, CCDC (1885563), as supplementary crystallographic data for the present paper. These data can be obtained free of charge from The Cambridge Crystallographic Data Center via www.ccdc.cam.ac.uk/data_request/cif. The graphics were drawn and additional structural calculations were performed by DIAMOND[5] software.

4. DNA Binding Studies

Having a good stability of complex **1** is crucial for the next biological studies, and it was conducted in saline.[3] The complex is soluble at 15 μM in Tris-HCl/NaCl buffer (10 mM Tris-HCl/50 mM NaCl, pH 7.40) containing 0.5% dimethylsulfoxide (DMSO). Then, UV-vis absorption spectra was recorded at a series of different time points (10 min, 2h, 24 h, 48 h and 72 h) respectively.

All experiments involving CT-DNA were determined in Tris-HCl buffer solution (5 mM Tris-HCl/50 mM NaCl, pH 7.40). The concentration of CT-DNA was determined by UV absorbance at 260 nm, taking 6600 $M^{-1}cm^{-1}$ as the molar absorption coefficient. The ratio of UV absorbance at 260 and 280 nm (A260/A280) was 1.85, indicating that the DNA solution was sufficiently free of protein.[4,5] Stock solution of CT-DNA was stored at 4 °C.

4.1 UV-Vis Absorption Spectra

The absorption spectra was performed by maintaining the concentrations of the complex (10 μM) with increasing concentration of DNA with the $R_{[DNA/complex\ \mathbf{1}]}$ = 0.25, 0.5, 1, 1.5, 2, 2.5, 3, 4, 5, 6, 7. The corresponding CT-DNA solution was deducted to eliminate the absorbance of DNA due to DNA at the measured wavelength. Before the absorption spectra was obtained, the complexes and DNA mixtures were incubated for 30 min at 37 ºC and the absorption spectra was scanned by a Specord 200 UV-visible spectrophotometer.

4.2 Emission Spectra

Emission spectroscopic studies of complex **1** with EB was performed using fluorescence spectroscopy. The EB was carried out in Tris-HCl/NaCl buffer (5 mM Tris-HCl, 50 mM NaCl, pH = 7.4). The DNA-EB solution (60 μM CT-DNA and 12 μ M EB) was incubated for 1 h at 37 ºC and then different concentrations (10-100 μM)were added into EB-DNA. After 3 h at 37 ºC, fluorescence quenching results were measured by recording the variation of fluorescence emission spectra (λ_{ex} = 490 nm, λ_{em} = 510.0–850.0 nm).

4.3 DNA Cleavage Studies

The cleavage studies of pBR322 supercoiled plasmid DNA was conducted by treating with different concentrations of the complex in a Tris-HCl buffer containing 50 mM Tris-HCl and 50 mM NaCl at pH 7.4 in the presence and absence of Vc, and the sample was incubated at 37 ℃ for 2 h, after that loading buffer was added. Then the samples were subjected to electrophoresis to seperate DNA fragments on 1% agarose gel at 80 V for 2 h. The stained electrophoresis bands by EB were visualized under a BIO-RAD Laboratories-Segrate gel imaging system.

5. Molecular docking analysis

The AutoDock 4.2 program was used to model the interaction between the complex and DNA. The X-ray crystal structure of the complex was selected in the subsequent docking and MD simulation as its large structure could not converge when using gaussian optimization algorithm. The DNA duplex of the sequence 5'-CGCGAATTCGCG-3' dodecamer was used for the docking study. For docking calculations, a Lamarckian genetic algorithm (LGA) was implemented with a total of 100 runs for the binding site. After the docking, the adducts with higher score was further studied by MD simulation using Amber 11.0 software.

6. Cell experiments

6.1 Cell Culture

The cisplatin resistant human cholangiocarcinoma cell line QBC939, esophagus tumor cell line EC109, liver tumor cell line SMMC7721 and normal liver cell LO-2 were purchased from KeyGEN bioTECH, and neuroblast tumor cell line SH-SY5Y were obtained from Xiamen University. The cells were routinely maintained in RPMI1640 (QBC939, EC109 and SMMC7721) and DMEM (SH-SY5Y) supplemented with 10% FBS (fetal bovine serum, Gemini), 100 U/mL streptomycin, and 100 ng/ mL penicillin at 37 °C under a humidified atmosphere containing 5% CO_2.

6.2 Cytotoxicity Assay

For the colorimetric MTT cytotoxicity test involving Cu (II) complex, a total of 6×10^3 cells/well were seeded in a 96-well plate and incubated in 5% CO_2/95% air at 37 °C for 24h, then the medium was eliminated and replaced with a fresh one (200 μL) containing the complex at five different concentrations. The test timescale (48 h) was established for each treatment. Finally, 20 μL of MTT solution (5 mg/mL in 1×PBS) was added in each well and left to incubate in the dark for 4h. The optical density of each well was measured at test wavelength of 492 nm using a microplate reader, the background absorbance of the media without cells + MTT was deducted from each well, and the control cells represented 100% viability.

6.3 Cellular Uptake Analysis

Exponentially growing SMMC7721 and LO-2 cells were seeded at a density of 6×10^5 cells in Petri dishes, after incubation for 24h at 37 °C, the cells were administered with 15 μM of copper complex and incubated for different time intervals. Then the cells were collected, and the nucleus and cytoplasm fractions of cells were extracted by a Cell Mitochondria Isolation Kit (Shanghai Beyotime Biological technology Co. Ltd). Briefly, the cells were firstly digested and washed twice with ice-cold PBS, then centrifuged at 600 g for 5 min. The sediment was gently suspended with cell mitochondria isolation reagent containing 1 mM PMSF in the ice for 10 min, then the cell suspension was transfered into a glass homogenizer (10 mL) with uniformly grinding 15 times. Again centrifuged at 600 g for 10 min at 4 °C, the supernatant was the cytoplasmic fraction and transferred to a clean microcentrifuge tube. The sediment at the bottom was the cell nucei. Both the nucleus and cytoplasm were mineralized with 65% HNO_3 (100 μL, 1 h), 30% H_2O_2 (50 μL, 1 h) and 36%-38% HCl (100 μL, 2 h) at 95 °C. And the total volume of each sample was diluted with ultrapure water to 1 mL, as cellular metal levels were shown as ng Cu per mL protein. An aliquot was used for protein concentration determined by the calibration curve created using Bradford method, and BSA as a reference standard. The copper concentration in each sample was determined by ICP-MS.

6.4 Comet Assay

SMMC7721 cells (2×10^5 cells) were treated with copper complex of varying concentrations for 12 h. Whereafter, cells were digested and resuspended with 1 mL PBS. And certain volume of cell suspension about 1000 cells were taken out to combine with 1% low-melting point agarose. The mix was then spread on slides which precoated with 0.5% normal melting point agarose, and then the slides were immersed into lysis buffer (2.5 M NaCl, 0.1 M EDTA, 0.01 M Tris base, 1% Triton-X100, 10% DMSO, pH 12) at 4 °C for 120 min. The slides were placed horizontally in an electrophoresis tank, submerging with alkaline electrophoresis buffer (0.3 M NaOH, 0.5 M EDTA) for 20 min at 4 °C, after which electrophoresis was carried out at 25 V for 30 min. Finally, the slides were neutralized with PBS, stained with 20 μL of ethidium bromide (50 μg/mL) at 37 °C

for 15 min and analyzed with a fluorescence microscope.

6.5 Cell Cycle Arrest

SMMC7721 cells were plated at 3×10^5/well in 6-well plates and incubated for 24 h. Then the medium replaced with complex **1** (0, 5, 10 and 15 μM). After incubation for 12 h, the cells were harvested. The cell staining procedure used the CycleTEST™ PLUS DNA Reagent Kit.

6.6 Analysis of Apoptosis

Determination of Mitochondrial Membrane Potential

SMMC7721 cells were seeded in 6-well plates and treated with different concentrations (0, 10 and 15 μM) for 12 h. The cells were harvested by trypsinization and then labeled with fluorescent dye rhodamine at 37 °C for 30 min in the dark. Then the cells were washed three times with RPMI 1640 and measured by flow cytometer.

ROS Generating

SMMC7721 cells were seeded in 6-well plates at a density of 3×10^5 cells per well and treated with complex **1** at different concentrations for 12 h. The fluorescent dye H_2DCF-DA was added to the medium with a final concentration of 10 μM to cover the cells at 37 °C for 20 min, then the cells were washed with RPMI 1640 for three times to eliminate dissociative fluorescent dye, and imaged with fluorescence microscope at 525 nm.

Flow Cytometric Analysis of Apoptosis

To further ascertain whether the complex induced cell death was caused due to an apoptotic pathway, we performed the Annexin V/PI dual assay to detect the presence of apoptotic cells after incubation with different concentrations of complex **1** (0, 10 and15 μM) for 12h. Then the cells was collected and washed with cold 1×PBS, resuspended in 200 μL binding buffer, and thereafter incubated with 5 μL Annexin V-FITC and 5 μL of PI solution for 15 min at 4 °C. Analysis was subsequently performed on flow cytometer.

6.7 Proteomics Analysis

Protein extraction and TMT Labeling

The cells were incubated with different concentrations (0, 5 and 10 μM) of complex **1** and disrupted by sonication on ice with 8 M urea/0.1 M Tris-HCl (pH 8.0)/1× Protease Inhibitor Cocktail (Roche). The protein was reduced with DTT for 2 h at 25 °C followed by alkylation with iodoacetamide for 30 min in the dark. The protein solution was diluted with TEAB and digested with trypsin at 37 °C overnight. The digestion was desalted on OASIS HLB column and peptides eluted with 60% acetonitrile were lyophilized via vacuum centrifugation. Then the dried peptides were dissolved with 100 mM TEAB buffer prior to labeled with Tandem Mass Tags (TMT). 100 μg of protein from each biological replicate of different experimental conditions was labeled with TMT six-plex® (Thermo Scientific) according to the manufacturer's instructions. The samples were labeled as follows: TMT-126/-127 was used for control samples, TMT-128/-129 for 5 μM treated samples and TMT-130/-131 for 10μM treated samples.

Peptide Pre-Fractionation Using High pH Reversed-Phase HPLC

Samples were fractionated using a Waters XBridge BEH130 C18 5 μm 4.6 × 250 mm column on a L-3000 HPLC System (Rigol) operating at 0.7 mL/min. All fractions were collected

at 90s intervals and concatenated into 12 post-fractions and lyophilized.

LC-MS/MS Analysis

All nanoLC-MS/MS experiments were performed on a Q Exactive equipped with an Easy n-LC 1000 HPLC system. The labeled peptides were loaded onto a fused silica trap column packed in-house with reversed phase silica and then separated on an C18 column packed with reversed phase silica. The MS analysis was performed with Q Exactive mass spectrometer. With the data-dependent acquisition mode, the MS data were acquired at a high resolution 70,000 (m/z 200) across the mass range of 300–1600 m/z.

Protein Identification and Quantification Analysis

The raw data from Q Exactive were analyzed with Proteome Discovery version 2.2.0.388 using Sequest HT search engine for protein identification and Percolator for FDR (false discovery rate) analysis. The Uniprot human protein database (updated 05-2017) was used for searching the data from human sample. FDR analysis was performed with Percolator, and FDR <1% was set for protein identification. The peptides confidence was set as high for peptides filter. Proteins quantification was performed using the ratio of the intensity of reporter ions from the MS/MS spectra. Only unique and razor peptides of proteins were selected for protein relative quantification.

References

1. G. M. Sheldrick, *Acta. Crystallogr. A.*, 2008, **64**, 112.
2. S. Lipstman, S. Muniappan and I. Goldberg, Cryst. Growth. Des., 2008, 8, 1683.
3. I. Yousuf, F. Arjmand, S. Tabassum, L. Toupet, R. A. Khanc, M. A. Siddiqui, *Dalton Trans.,* 2015, **44**, 10330.
4. J. Marmur, *J. Mol. Bio.*, 1961, **3**, 208.
5. M. Reichmann, S. Rice, C. Thomas and P. Doty, *J. Am. Chem. Soc.*, 1954, **76**, 3047.

7. Supplementary Spectra and Charts

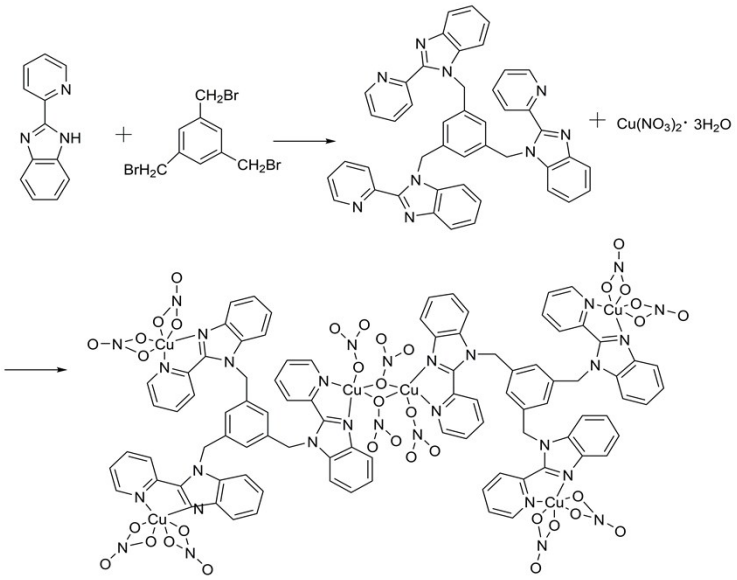

Scheme S1. The routine of $Cu_6(tpbb)_2(NO_3)_{12}$ synthesis

Table S1. Crystallographic data and structure refinement parameters for the complex

Complex	**1**
Formula	$Cu_3C_{45}H_{33}N_{15}O_{18}$
Formula weight	1262.48
Temp(K)	293(2)
λ (Mo Cu/ Kα), Å	1.5418
Crystal system	monoclinic
Space group	$P2_1/n$
a (Å)	12.1943(4)
b (Å)	24.9979(10)
c (Å)	19.9314(7)
α(deg)	90.00
β(deg)	94.521(3)
γ(deg)	90.00
V ($Å^3$)	6056.8(4)
Z	4
F(000)	2556.0
θ range for data collection (deg)	8.088~ 134.16
Final R1, [a]wR2[b]	0.0997, 0.2623
goodness-of-fit on F^2	1.025

Table S2. Selected bond lengths (Å) and angles (°)for the complex

Bond lengths			
Cu(1)–O(4)	1.981(5)	Cu(1)–O(4) #1	2.412(6)
Cu(1)–N(2)	1.956(6)	Cu(1)–O(3)	1.959(7)
Cu(1)–N(1)	2.020(8)	Cu(3)–N(8)	1.961(7)
Cu(3)–N(7)	1.989(8)	Cu(3)–O(16)	2.016(8)
Cu(3)–O(13)	1.952(8)	Cu(2)–N(4)	2.028(8)
Cu(2)–N(5)	1.954(8)	Cu(2)–O(8)	1.991(8)
Cu(2)–O(7)	2.440(9)	Cu(2)–O(10)	1.987(14)
Bond angles			
O(4)–Cu(1)–O(4) #1	73.1(2)	O(4)–Cu(1)–N(1)	93.3(3)
N(2)–Cu(1)–O(4) #1	99.1(2)	N(2)–Cu(1)–O(4)	170.4(2)
N(2)–Cu(1)–O(3)	95.1(3)	N(2)–Cu(1)–O(1)	81.7(3)
O(3)–Cu(1)–O(4)#1	92.6(3)	O(3)–Cu(1)–O(4)	90.8(3)
O(3)–Cu(1)–N(1)	172.9(3)	N(1)–Cu(1)–O(4)#1	94.1(3)
N(8)–Cu(3)–N(7)	81.9(3)	N(8)–Cu(3)–O(16)	94.3(3)
N(7)–Cu(3)–O(16)	154.0(3)	O(13)–Cu(3)–N(8)	170.9(4)
O(13)–Cu(3)–N(7)	96.7(4)	O(13)–Cu(3)–O(16)	90.8(3)
N(4)–Cu(2)–O(7)	93.8(4)	N(5)–Cu(2)–N(4)	80.6(3)
N(5)–Cu(2)–O(8)	173.0(3)	N(5)–Cu(2)–O(7)	120.1(3)
N(5)–Cu(2)–O(10)	95.5(5)	O(8)–Cu(2)–N(4)	94.1(3)
O(8)–Cu(2)–O(7)	55.4(3)	O(10)–Cu(2)–N(4)	168.9(6)
O(10)–Cu(2)–O(8)	90.5(5)	O(10)–Cu(2)–O(7)	97.2(6)

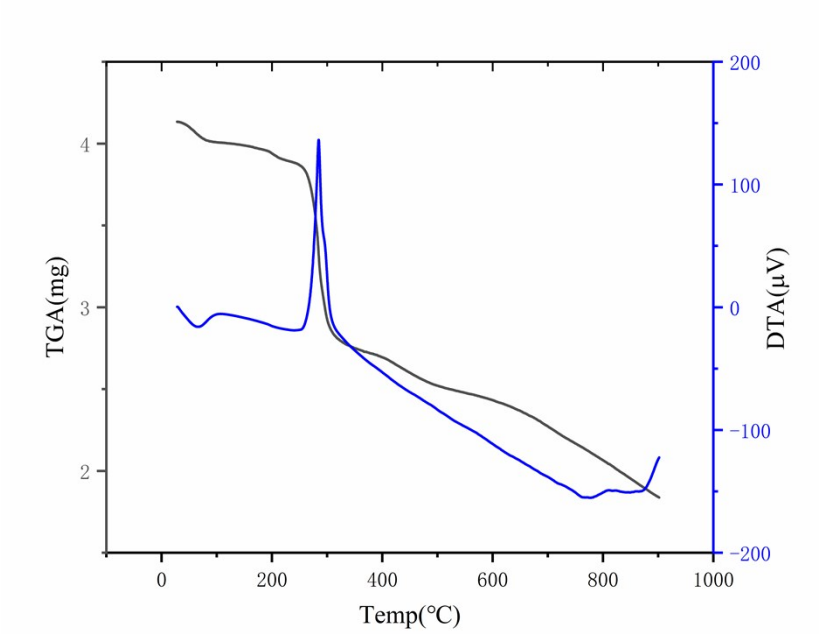

Figure S1. Thermogravimetric analysis of complex **1.**

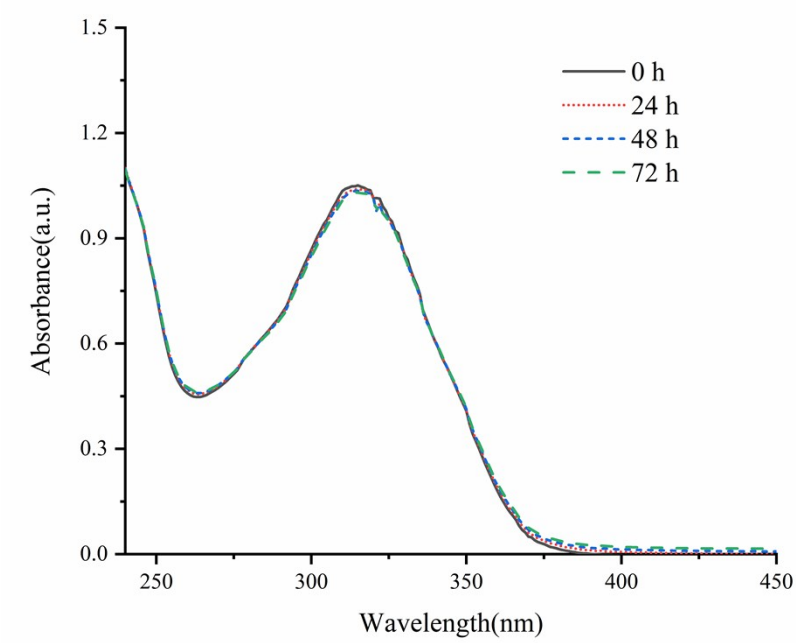

Figure S2. Absorption spectra of complex **1** with 10 μM in 0.5% DMSO-Tris-HCl/NaCl buffer (25 °C) at different time points measured by UV-Vis spectrophotometer.

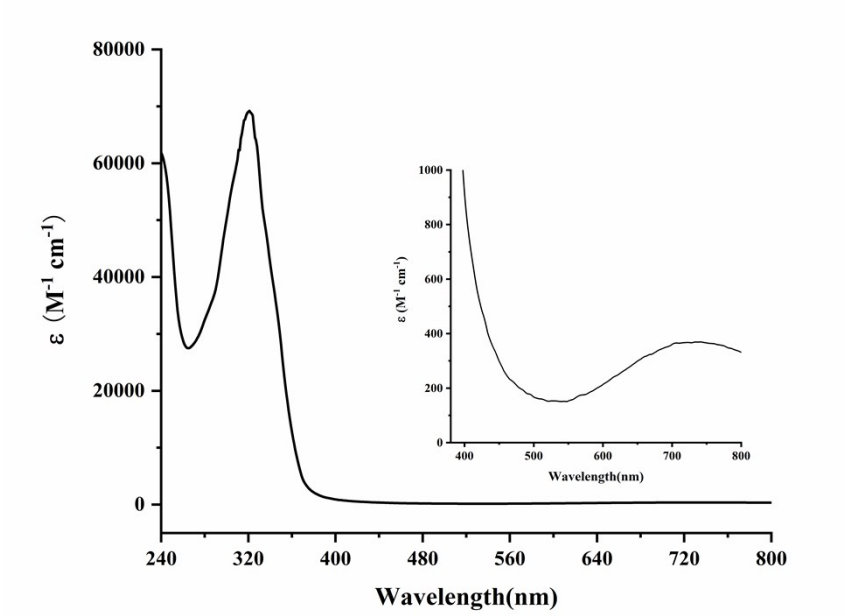

Figure S3. Absorption spectrum of complex **1** with 45 μM in DMSO-Tris-HCl/NaCl buffer (25 °C) in the UV-Vis region (240-800 nm). The inset shows the optical band in the visible region (380-800 nm) in which the d-d transition can be seen.

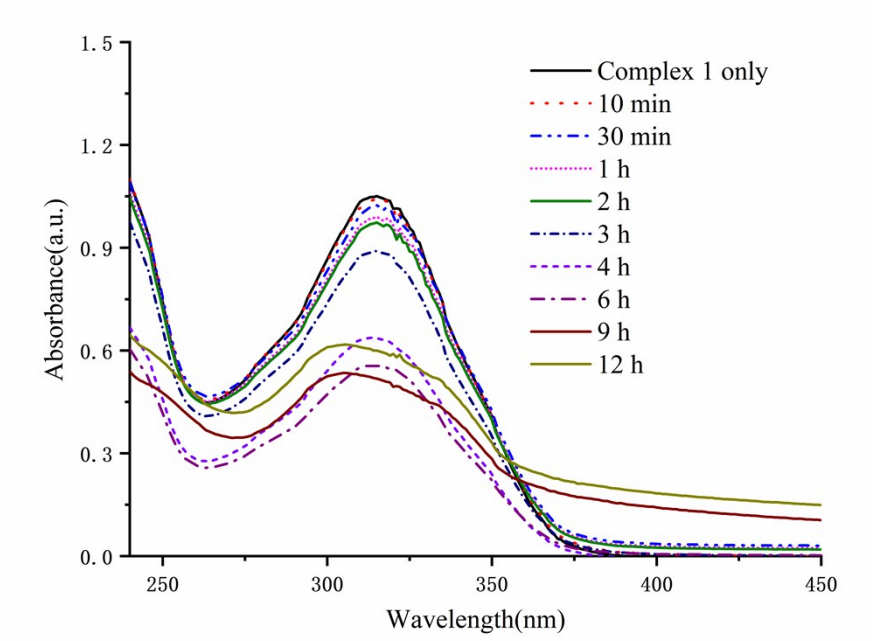

Figure S4. Absorption spectra of complex **1** in 0.5% DMSO-Tris-HCl/NaCl buffer containing 2mM GSH (25 °C) at different time points.

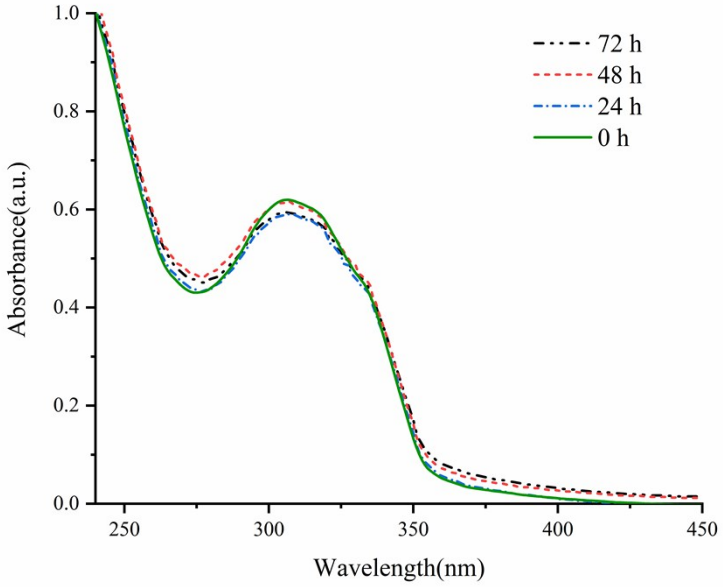

Figure S5. Absorption spectra of complex **1** in RPMI 1640 supplemented with 10% FBS (37 °C) at different time points.

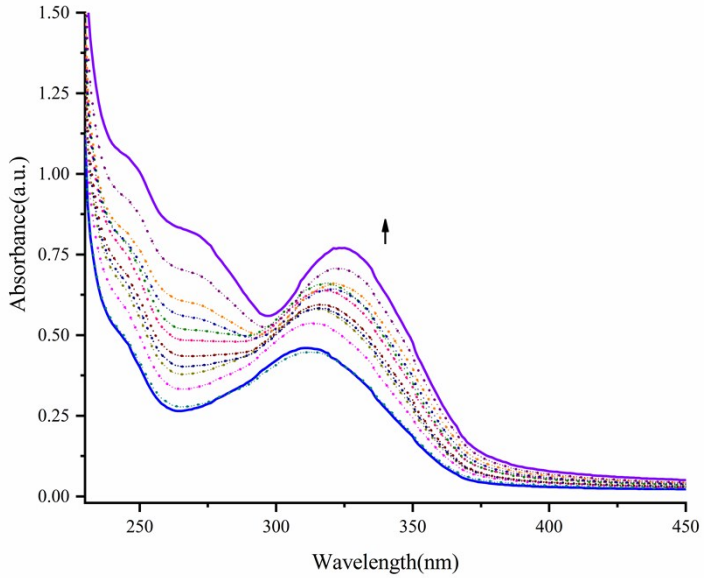

Figure S6. Absorption spectra of in a 5 mM Tris HCl/50 mM NaCl buffer at pH=7.2 with increasing amounts of DNA, ([CT-DNA]/[complex]: 0.25, 0.5, 1, 1.5,2,2.5, 3, 4, 5, 6,7)

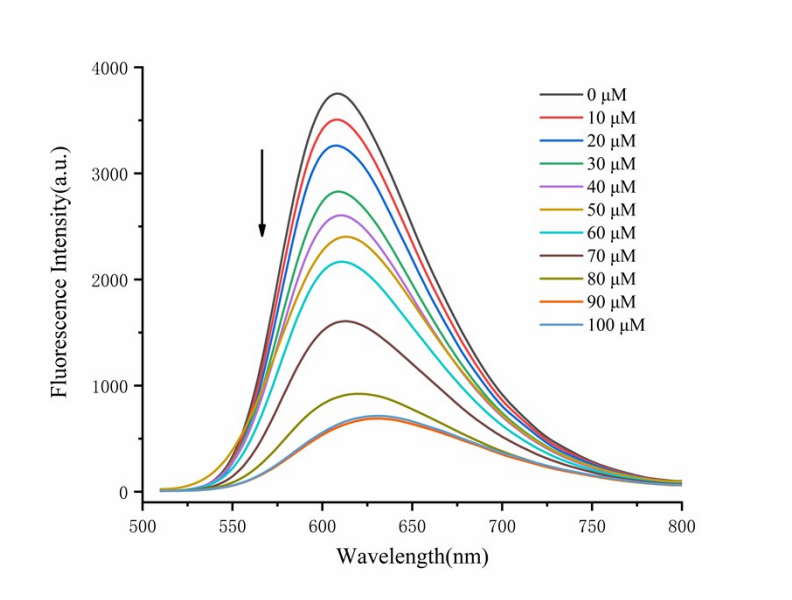

Figure S7. Effect of the addition of complex **1** on the emission intensity of the CT-DNA bound EB at different concentrations in a 5mM Tris-HCl/50mM NaCl buffer, pH7.2 at 37 ℃.

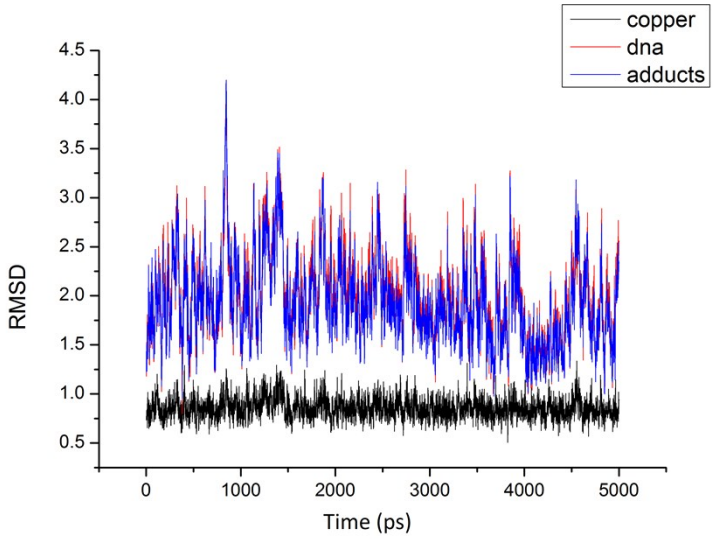

Figure S8. The RMSD value change using molecular dynamics simulations using AMBER11 software

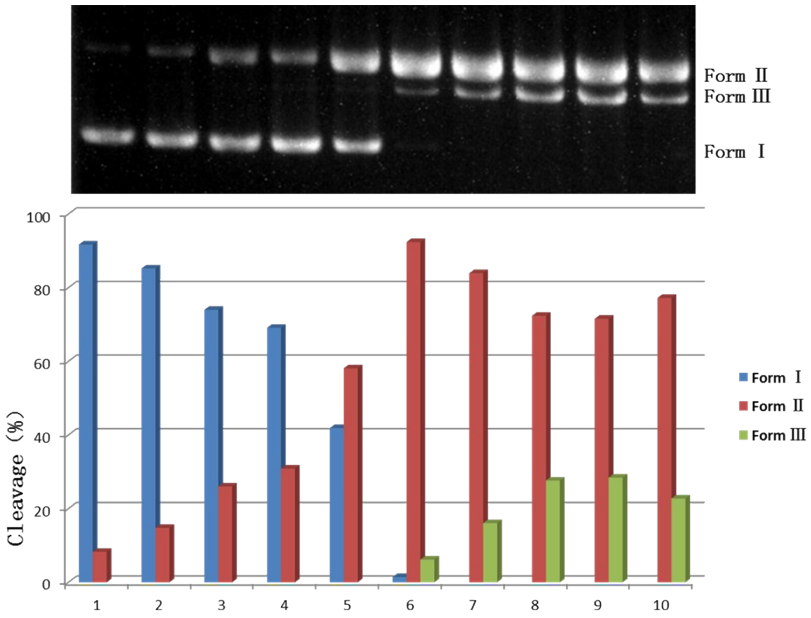

Figure S9. The cleavage patterns of the agarose gel electrophoresis and corresponding cleavage extent for pBR322 plasmid DNA. Lane 1, DNA ; Lane 2, DNA+ 1(50 μM); Lane 3, DNA + Vc ; Lane 4, DNA + 1(5 μM); Lane 5, DNA + Vc + 1(10 μM); Lane 6, DNA + Vc + 1(15 μM); Lane 7, DNA + Vc + 1(20 μM), Lane 8, DNA + Vc + 1(30μM); Lane 9, DNA + Vc + 1(40 μM); Lane 10, DNA + Vc + 1(50 μM).

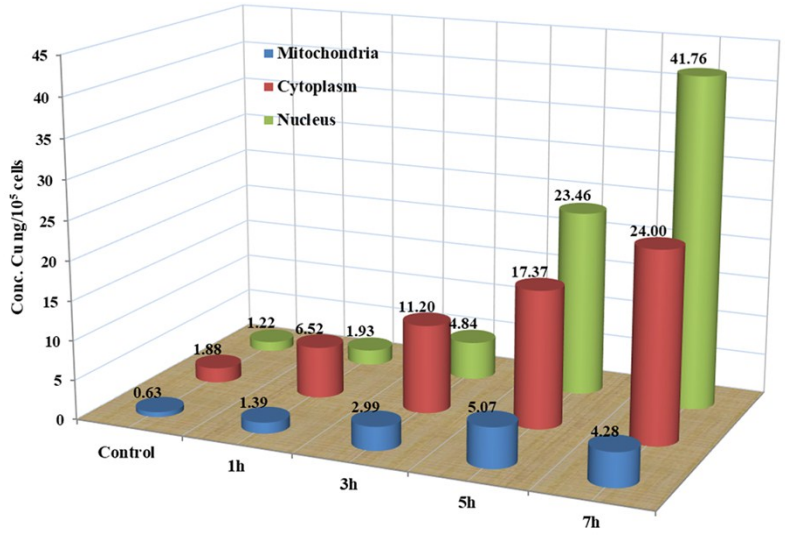

Figure S10. SMMC7721 cells treated by 15 μM complex **1** at different time intervals. Copper content in 10^5 cells distributed in the nucleus, cytoplasm and mitochondria detected by ICP-MS.

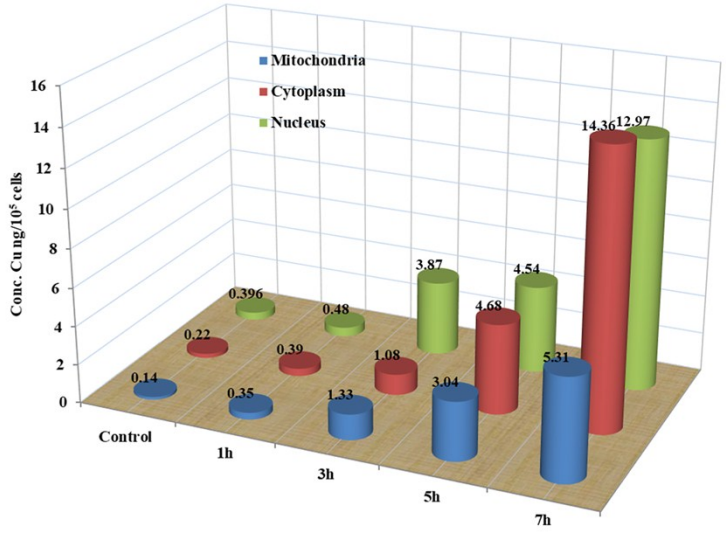

Figure S11. LO-2 cells treated by 15 μM complex **1** at different time intervals. Copper content in 10^5 cells distributed in the nucleus, cytoplasm and mitochondria detected by ICP-MS.

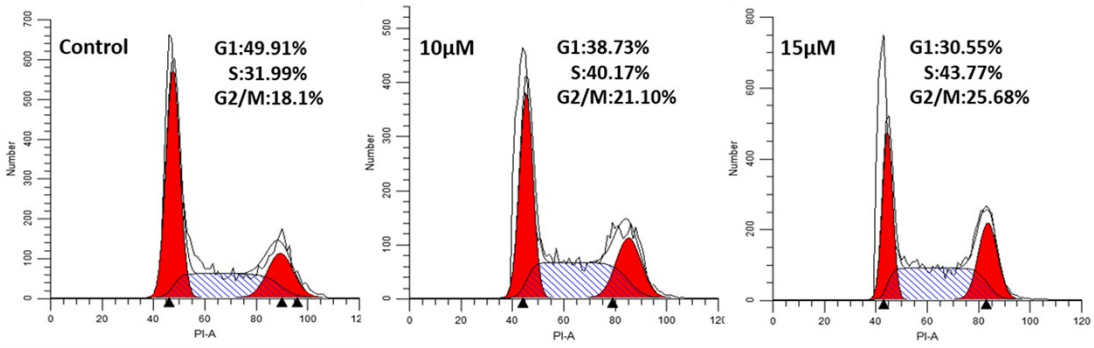

Figure S12. Cell cycle distribution in SMMC7721 cells after treated by different concentration of complex **1**.

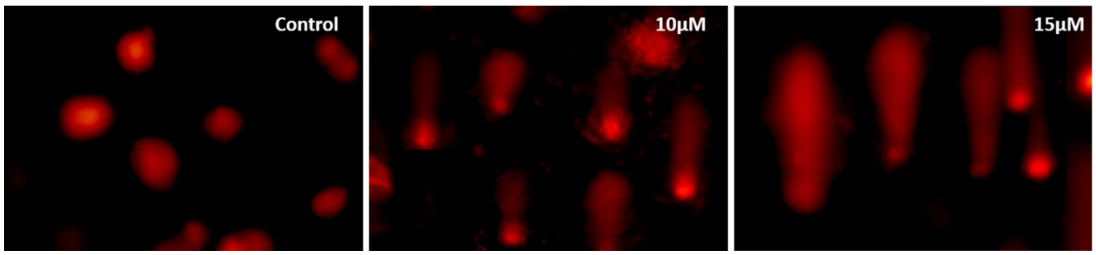

Figure S13. Chromosomal DNA strand breaks in SMMC7721 cells as detected by comet assay.

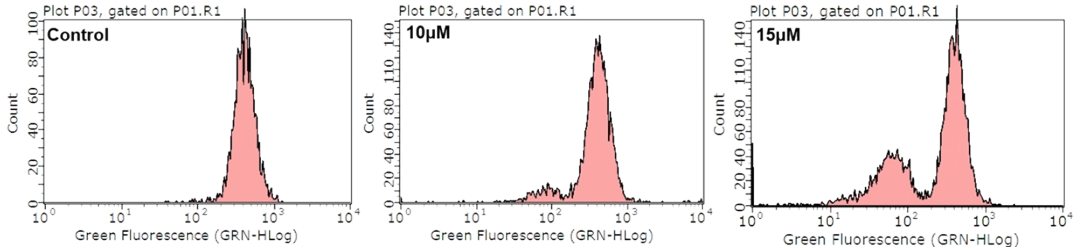

Figure S14. Effect of complex **1** on the ΔΨm of SMMC7721 cells for 24 h

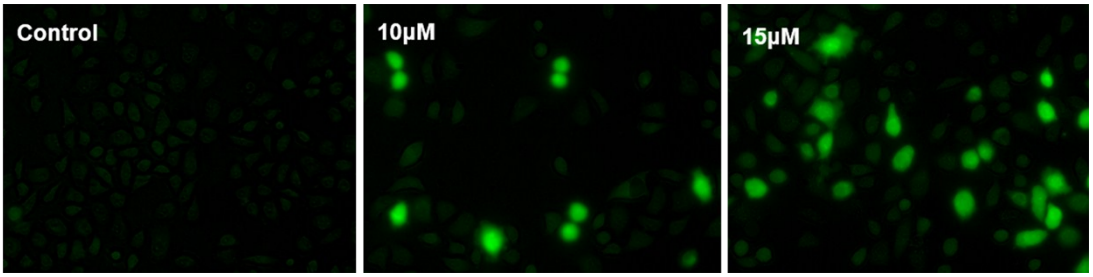

Figure S15. ROS generation induced by complexes with different concentrations

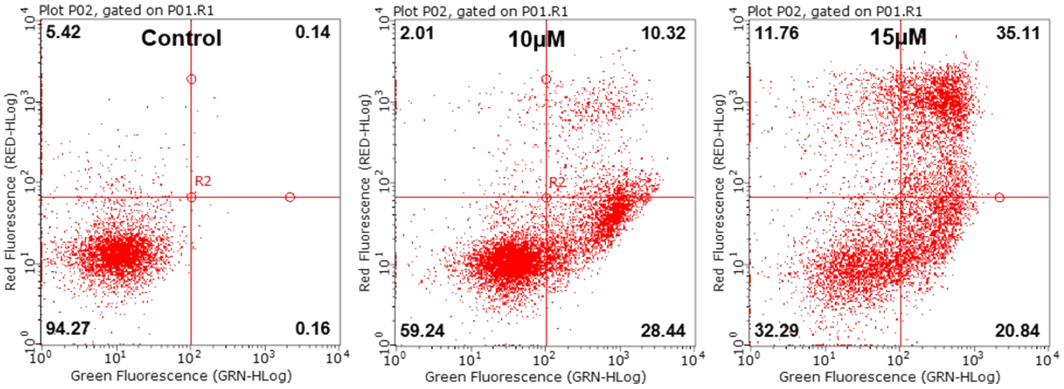

Figure S16. Apoptosis in SMMC7721 induced by different concentrations of complex **1**

Table S3. Proteins showing consistently expressional changes in two group cells

Accession	Protein name	Gene name	Abundance ratio (02) / (01)	Abundance ratio (03) / (01)
O15379-2	Isoform 2 of Histone deacetylase 3	HDAC3	0.305	0.416
Q01432-4	Isoform 2 of AMP deaminase 3	AMPD3	0.308	0.475
Q9GZP8	Immortalization up-regulated protein	IMUP	0.35	0.468
Q96D05-2	Isoform 2 of Uncharacterized protein C10orf35	C10orf35	0.361	0.432
Q9NRY2	SOSS complex subunit C	INIP	0.389	0.436
Q6ZN08	Putative zinc finger protein 66	ZNF66	0.398	0.359
Q9NQ50	39S ribosomal protein L40, mitochondrial	MRPL40	0.419	0.605
Q9Y2D2-2	Isoform 2 of UDP-N-acetylglucosamine transporter	SLC35A3	0.437	0.576
Q9NR28	Diablo homolog, mitochondrial	DIABLO	0.44	0.609
H3BN98		Uncharacterized	0.453	0.531
P61769	Beta-2-microglobulin	B2M	0.46	0.611
Q8NBM4	Ubiquitin-associated domain-containing protein 2	UBAC2	0.46	0.76
P62987 P05534	Ubiquitin-60S ribosomal protein L40	UBA52	0.461	0.58
P18077	60S ribosomal protein L35a	RPL35A	0.534	0.598
B4DL54	Protein CHURC1-FNTB	CHURC1-FNTB	0.473	0.561
Q9UEG4	Zinc finger protein 629	ZNF629	0.549	0.605
O43493	Trans-Golgi network integral membrane protein 2	TGOLN2	0.534	0.495
O14770	Homeobox protein Meis2	MEIS2	0.529	0.468
C9JEH3	Angio-associated migratory cell protein	AAMP	0.595	0.55
P51397	Death-associated protein 1	DAP	0.549	0.583
Q8IWA5-2	Isoform 2 of Choline transporter-like protein 2	SLC44A2	0.551	0.566
P13473-3	Isoform LAMP-2C of Lysosome-associated membrane glycoprotein 2	LAMP2	0.607	0.615
Q00535	Cyclin-dependent-like kinase 5	CDK5	0.61	0.62
Q9NQX6	Zinc finger protein 331	ZNF33	0.691	0.566
H7C561	Splicing factor 1 (Fragment)	SF1	0.617	0.706
O75157	TSC22 domain family protein 2	TSC22D2	0.628	0.739
Q5VZF2	Muscleblind-like protein 2	MBNL2	0.505	0.272
Q01628	Interferon-induced transmembrane protein	IFITM3	0.614	0.634
A0A075B6T4	Kelch repeat and BTB domain-containing protein 4	KBTBD4	0.525	0.486
Q9H0X4	Protein FAM234A	FAM234A	0.683	0.701
Q02543	60S ribosomal protein L18a	RPL18A	0.718	0.74
P31151	Protein S100-A7	S100A7	0.734	0.636

P55061-2	Isoform 2 of Bax inhibitor 1	TMBIM6	0.654	0.683
P07305	Histone H1.0	H1F0	0.561	0.47
Q13547	Histone deacetylase 1	HDAC1	0.598	0.593
Q5JTD0-2	Isoform 2 of Tight junction-associated protein 1	TJAP1	0.723	0.736
B7Z4C8	60S ribosomal protein L31	RPL31	0.685	0.66
P61254	60S ribosomal protein L26	RPL26	0.746	0.767
Q9NX55	Huntingtin-interacting protein K	HYPK	0.708	0.589
P49591	Serine--tRNA ligase, cytoplasmic	SARS	0.689	0.666
P61244	Protein max	MAX	0.697	0.727
Q7Z4H8	KDEL motif-containing protein 2	KDELC2	0.69	0.569
O60337	E3 ubiquitin-protein ligase MARCH6	MARCH6	0.74	0.66
P04732	Metallothionein-1E	MT1E	0.721	0.722
Q8WVV4-1	Isoform 1 of Protein POF1B	POF1B	0.629	0.63
P41236	Protein phosphatase inhibitor 2	PPP1R2	0.751	0.764
P09669	Cytochrome c oxidase subunit 6C	COX6C	0.772	0.731
P36954	DNA-directed RNA polymerase II subunit RPB9	POLR2I	0.626	0.639
Q2TAL8	Glutamine-rich protein 1	QRICH1	0.769	0.737
Q9Y324	rRNA-processing protein FCF1 homolog	FCF1	0.735	0.632
Q8IUE6	Histone H2A type 2-B	HIST2H2AB	0.599	0.083
P46776	60S ribosomal protein L27a	RPL27A	0.756	0.785
Q9UPY8	Microtubule-associated protein RP/EB family member 3	MAPRE3	0.759	0.709
P50238	Cysteine-rich protein 1	CRIP1	0.767	0.702
P62491	Ras-related protein Rab-11A	RAB11A	0.669	0.765
Q8NI22	Multiple coagulation factor deficiency protein 2	MCFD2	0.76	0.516
Q13131-2	Isoform 2 of 5'-AMP-activated protein kinase catalytic subunit alpha-1	PRKAA1	0.783	0.726
A6NGJ0	Dynein light chain Tctex-type 3	DYNLT3	0.764	0.624
P30530	Tyrosine-protein kinase receptor UFO	AXL	0.782	0.719
P04080	Cystatin-B	CSTB	0.762	0.685
Q8N4J0	Carnosine N-methyltransferase	CARNMT1	0.746	0.753
Q17RN3	Protein FAM98C	FAM98C	0.669	0.743
Q9Y5Z0	Beta-secretase 2	BACE2	0.708	0.714
Q9H467	CUE domain-containing protein 2	CUEDC2	0.797	0.606
Q9H3Z4	DnaJ homolog subfamily C member 5	DNAJC5	0.755	0.752
A0A0C4DGV4	Hepatitis B virus x interacting protein	LAMTOR5	0.735	0.651
P02462	Collagen alpha-1(IV) chain	COL4A1	0.69	0.569
O15121	Sphingolipid delta(4)-desaturase DES1	DEGS1	0.746	0.728
G8JLA2	Myosin light polypeptide 6	MYL6	0.784	0.627

P62857	40S ribosomal protein S28	RPS28	2.364	1.863
A0A0C4DFZ2	Arylsulfatase A	ARSA	1.678	1.462
Q8TA94	Zinc finger protein 563	ZNF563	2.062	2.073
O94864	STAGA complex 65 subunit gamma	SUPT7L	1.707	1.404
Q86YZ3	Hornerin	HRNR	1.843	1.907
O00622	Protein CYR61	CYR61	1.326	1.573
A0A087WYF7	MICOS complex subunit	APOOL	1.640	1.599
Q8WUY8	N-acetyltransferase 14	NAT14	1.630	1.381
P42684	Abelson tyrosine-protein kinase 2	ABL2	1.726	1.618
P61587	Rho-related GTP-binding protein RhoE	RND3	1.759	4.853
P02538	Keratin, type II cytoskeletal 6A	KRT6A	1.585	1.276
H0Y962	Carbonyl reductase family member 4 (Fragment)	CBR4	1.473	1.283
Q9UFB7	Zinc finger and BTB domain-containing protein 47	ZBTB47	1.610	1.657
H0YL33	Annexin (Fragment)	ANXA2	1.862	1.581
P08779	Keratin, type I cytoskeletal 16	KRT16	1.394	1.259
Q92802-3	Isoform 3 of NEDD4-binding protein 2-like 2	N4BP2L2	1.528	1.581
J3KP97	Coiled-coil domain-containing protein 18 (Fragment)	CCDC18	1.375	1.756
P13726	Tissue factor	F3	1.277	1.891
Q14697	Neutral alpha-glucosidase AB	GANAB	1.606	3.079
A0A0U1RQE4	SH3 domain-containing protein 19	SH3D19	1.368	1.319
O60356-2	Isoform 2 of Nuclear protein 1	NUPR1	1.642	2.43
B0I1T2	Unconventional myosin-Ig	MYO1G	1.334	1.715
A0A087WWB6	Transgelin	TAGLN3	1.337	2.439
P83110	Serine protease HTRA3	HTRA3	1.266	2.027
Q9GZV5	WW domain-containing transcription regulator protein 1	WWTR1	1.275	1.332
Q06609-4	Isoform 4 of DNA repair protein RAD51 homolog 1	RAD51	1.376	1.391
Q5NDL2	EGF domain-specific O-linked N-acetylglucosamine transferase	EOGT	1.354	1.563
P15407	Fos-related antigen 1	FOSL1	1.265	2.034
P0CG39	POTE ankyrin domain family member J	POTEJ	1.296	2.238

Table S4. Top 10 enriched Gene ontology terms for cellular component, molecular function and biological

process identified using at least two techniques

GO term ID	GO terms	Observed gene count
	CELLULAR COMPONENT	
GO:0005622	intracellular region	227
GO:0032991	macromolecular complex	107
GO:0005634	nucleus	71
GO:0005886	Plasma membrane	37
GO:0005783	endoplasmic reticulum	21
GO:0005856	cytoskeleton	19
GO:0005739	mitochondrion	16
GO:0005794	Golgi apparatus	15
GO:0005694	chromosome	9
GO:0042175	Nuclear outer membrane-endoplasmic reticulum membrane network	9
	MOLECULAR FUNCTION	
GO:0003824	catalytic activity	171
GO:0005515	protein binding	109
GO:0003676	nucleic acid binding	65
GO:0003735	Structural constituent of ribosome	22
GO:0004871	Signal transducer activity	16
GO:0005200	Structural constituent of cytoskeleton	15
GO:0000166	nucleotide binding	9
GO:0003682	chromation binding	8
GO:0005509	calcium binding	6
GO:0008289	lipid binding	5
	BIOLOGICAL PROCESS	
GO:0008152	Metabolic process	234
GO:0071840	Cellular component organization or biogenesis	83
GO:0007154	Cell communication	75
GO:0050896	Response to stimulus	71
GO:0050789	Regulation of biological process	65
GO:0007040	Biosynthesis process	67
GO:00032502	Developmental process	49
GO:0007040	Cell cycle	33
GO:0030154	Cell differentiation	19
GO:0006928	Cellular component movement	13

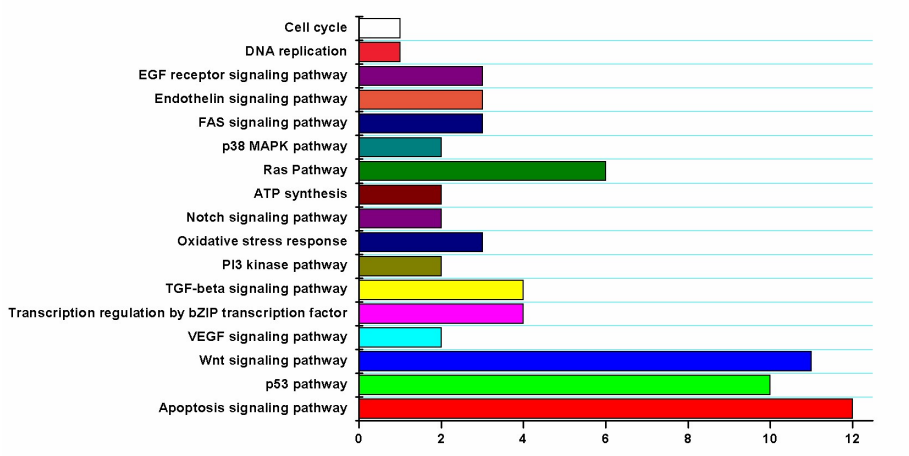

Figure S17. KEGG pathway analysis of identified 117 proteins involved in SMMC7721 cells treated with complex **1**.